

MICROCOPY RESOLUTION TEST CHART
NATIONAL BUREAU OF STANDARDS-1963-A

AT-E 430598

FILE

12
13 5-

AD

AD A 098660

MEMORANDUM REPORT ARBRL-MR-03082

STRAIN-GAGE TECHNIQUES FOR STUDIES OF
PROJECTILE BEHAVIOR DURING PENETRATION

G. E. Hauver
A. Melani

February 1981

DIC
S MAY 8 1981 D

A



US ARMY ARMAMENT RESEARCH AND DEVELOPMENT COMMAND
BALLISTIC RESEARCH LABORATORY
ABERDEEN PROVING GROUND, MARYLAND

Approved for public release; distribution unlimited.

DIC FILE COPY

81 4 16 005

Destroy this report when it is no longer needed.
Do not return it to the originator.

Secondary distribution of this report by originating
or sponsoring activity is prohibited.

Additional copies of this report may be obtained
from the National Technical Information Service,
U.S. Department of Commerce, Springfield, Virginia
22161.

The findings in this report are not to be construed as
an official Department of the Army position, unless
so designated by other authorized documents.

*The use of trade names or manufacturers' names in this report
does not constitute endorsement of any commercial product.*

REPORT DOCUMENTATION PAGE		READ INSTRUCTIONS BEFORE COMPLETING FORM
1. REPORT NUMBER MEMORANDUM REPORT ARBRL-MR-03082	2. GOVT ACCESSION NO. AD-A0 98 660	3. RECIPIENT'S CATALOG NUMBER
4. TITLE (and Subtitle) Strain-Gage Techniques for Studies of Projectile Behavior During Penetration	5. TYPE OF REPORT & PERIOD COVERED Final	
	6. PERFORMING ORG. REPORT NUMBER	
7. AUTHOR(s) G. E. Hauver and A. Melani	8. CONTRACT OR GRANT NUMBER(s)	
9. PERFORMING ORGANIZATION NAME AND ADDRESS US Army Ballistic Research Laboratory ATTN: DRDAR-BLT Aberdeen Proving Ground, MD 21005	10. PROGRAM ELEMENT, PROJECT, TASK AREA & WORK UNIT NUMBERS 1L161102AH43	
11. CONTROLLING OFFICE NAME AND ADDRESS US Army Armament Research & Development Command US Army Ballistic Research Laboratory (DRDAR-BL) Aberdeen Proving Ground, MD 21005	12. REPORT DATE FEBRUARY 1981	
	13. NUMBER OF PAGES 43	
14. MONITORING AGENCY NAME & ADDRESS (if different from Controlling Office)	15. SECURITY CLASS. (of this report) Unclassified	
	15a. DECLASSIFICATION/DOWNGRADING SCHEDULE	
16. DISTRIBUTION STATEMENT (of this Report) Approved for Public Release; Distribution Unlimited		
17. DISTRIBUTION STATEMENT (of the abstract entered in Block 20, if different from Report)		
18. SUPPLEMENTARY NOTES		
19. KEY WORDS (Continue on reverse side if necessary and identify by block number) Penetration Long-Rod Projectiles Strain Gages		
20. ABSTRACT (Continue on reverse side if necessary and identify by block number)		bet/2972
The behavior of long steel rods during the penetration of steel armor is being examined by strain measurements performed with foil resistance gages. Experiments in this investigation have employed both forward-ballistic and reverse-ballistic techniques. These techniques are described, and their advantages and disadvantages are discussed. Test data have been examined by a simple-wave analysis, and analytical results are discussed within the context of experimental problems. Preliminary efforts to assess the validity of		

UNCLASSIFIED

SECURITY CLASSIFICATION OF THIS PAGE(When Data Entered)

20. (Continued)

measurements and analysis are described.

UNCLASSIFIED

SECURITY CLASSIFICATION OF THIS PAGE(When Data Entered)

TABLE OF CONTENTS

	<u>Page</u>
TABLE OF CONTENTS.	3
LIST OF ILLUSTRATIONS.	4
I. INTRODUCTION	7
II. FORWARD-BALLISTIC TECHNIQUE.	7
A. Probes and Contacts.	7
B. Experimental Arrangement	8
C. Strain Gages	11
D. Strain-Gage Circuit.	12
E. Sabot Orientation.	12
III. REVERSE-BALLISTIC TECHNIQUE.	12
IV. DISCUSSION OF PROBLEM AREAS AND RESULTS.	14
A. Target Ejecta.	15
B. Signal Loss.	15
C. Signal Distortion and Electrical Noise	19
D. Number of Gages.	27
E. Data Reduction	28
F. Reliability of Data and Analysis	33
V. SUMMARY AND CONCLUSIONS.	37
REFERENCES	40
DISTRIBUTION LIST.	41

A

LIST OF ILLUSTRATIONS

<u>Fig. No.</u>		<u>Page</u>
1	Configurations of probes and contacts tested to determine if a low-resistance electrical path could be maintained between stationary probes and contacts moving at ballistic velocity.	9
2	Experimental arrangement for forward-ballistic experiments.	10
3	Bridge circuit for strain-gage measurements.	13
4	Experimental arrangement for reverse-ballistic experiments.	16
5	Photographic study of target ejecta produced when a long steel rod strikes steel armor at a velocity of 1000 m/s.	17
6	Strain/time records from an early forward-ballistic experiment with strain gages located 20, 40, and 60mm from the tip of the rod.	20
7	Stress/strain and particle velocity/strain relationships obtained by a simple-wave analysis of strain/time records which included those shown in Figure 6	21
8	Displacements, relative to the sabot, that occur when the steel rod decelerates after impact in the forward-ballistic experiment at 1000 m/s	22
9	Time/distance diagram in laboratory coordinates, showing a steel rod impacting a steel target at 1000 m/s	23
10	Strain/time records from a reverse-ballistic experiment in which a stationary steel rod was impacted by a steel target launched at 710 m/s	24
11	Stress/strain and particle velocity/strain relationships obtained by a simple-wave analysis of the strain/time records shown in Figure 10	25
12	Time/distance diagram in laboratory coordinates, showing a steel rod impacting a steel target at 710 m/s.	26
13	Oscilloscope records	29
14	Typical distortion in an oscilloscope record	31

<u>Fig. No.</u>		<u>Page</u>
15	Oscilloscope record with features of the time calibration identified.	32
16	Reverse-ballistic arrangement used for optical measurements of rod displacement during penetration.	34
17	Photographic record of rod displacement during penetration (reverse-ballistic experiment)	35
18	Displacement/time relationship, comparing displacement measured optically with displacement calculated from strain measurements	36
19	Comparison of displacements at the lower impact velocity of 450 m/s.	38

I. INTRODUCTION

Bluhm¹, in 1956, reported the results of a study in which thin plates were impacted against stationary projectiles instrumented with wire resistance strain gages. Similar reverse-ballistic tests have since been reported by others including Araj² and Lascher, Henderson, and Maynard³. Reverse ballistics offers the advantage of a stationary projectile which may be easily instrumented with strain gages. However, the diameter of the impacting target is limited by the gun bore and the impact velocity is limited by the target mass, and these limitations may be severe. Forward ballistics, in contrast, imposes few restrictions on the target, but the moving projectile is more difficult to instrument. Both forward-ballistic and reverse-ballistic techniques have been used for instrumented penetrator studies at the Ballistic Research Laboratory (BRL). This report describes both techniques, discusses problem areas which have been encountered, and presents a preliminary assessment of results.

II. FORWARD-BALLISTIC TECHNIQUE

Forward ballistics refers to the usual ballistic approach in which projectiles are launched at stationary targets. Projectiles are commonly much less massive than the target so this approach should permit impact velocities higher than those which can be achieved when the target is launched in reverse-ballistic studies. The objective of the BRL investigation has been to examine the strain response of long steel rods as they penetrate steel armor. The higher impact velocities possible with forward ballistics made this technique desirable but presented the problem of instrumenting a moving rod.

A. Probes and Contacts.

A way of monitoring gage resistance is necessary if rods instrumented with strain gages are launched at stationary targets. Figure 1 shows configurations which were tested to determine if a low-resistance path could be maintained between a stationary probe and an electrical contact moving at ballistic velocity. Metal plates which served as contacts were mounted on the front surface of a plastic sabot. These contacts were connected by a resistor which simulated a strain gage and were isolated

¹J. I. Bluhm, "Stresses in Projectiles During Penetration", *Proc. Soc. Exptl. Stress Analysis*, Vol. 13, 1956, pp. 167-182.

²Visi Araj, "An Investigation of Forces on a Projectile During Perforation of Thin Aluminum Plates", *Masters Thesis, Air Force Inst. Tech.*, June 1971.

³F. R. Lascher, D. Henderson, and D. Maynard, "Determination of Penetration Forcing Function Data for Impact Fuzes", *Avco Systems Division, Wilmington, Mass., Technical Report AVSD-0306-75-RR, January 1975.*

by a plastic shield which was intended to prevent electrical conduction through surface ejecta. Soft cylindrical probes (A) and folding probes (B) accumulated on the surface of thick contacts and were found to provide a high-resistance path which, in the case of folding probes, varied by as much as 10 ohms. Lower resistances were achieved with tapered probes (C and D) which pierced the contacts, and thinner contacts produced smaller variations in resistance. The results suggested that resistance and its variation depended on the amount of severely deformed metal in the conducting path, and the combination of tapered steel probes and thin steel contacts decreased the resistance variations to approximately 0.2 ohm. Most of this 0.2 ohm variation was later attributed to the influence of mechanical disturbances on the carbon load resistor which was connected between contacts on the sabot surface. When this resistor was relocated at the back end of a stationary probe, most of the variation disappeared. Occasional variations in resistance during a measurement could usually be attributed either to poor probe alignment, or to beginning a measurement too soon after the probe pierced the contact, when the interface area was small.

B. Experimental Arrangement.

Tapered steel probes and thin steel contacts were incorporated into the experimental arrangement used for early experiments. This experimental arrangement is shown in Figure 2. In this arrangement a steel rod, 8.1mm in diameter and 250mm in length, is launched in a sabot which is constructed primarily of polypropylene. The base of the rod is supported by an aluminum-alloy plate, and mid-rod support is provided by a phenolic guide at the front surface of the sabot. The rod is instrumented with either four or six strain gages, and each strain gage is connected by leadwires to a pair of 0.4mm thick steel contacts located on the front surface of the sabot. Leadwires, like the strain gages, are bonded to the rod surface. One steel contact is common to all gages, so seven contacts are required for six gages. A cavity was placed behind each contact after measurements suggested that the rod might be perturbed when sabot material was displaced by the probes. Probes are allowed to penetrate several millimetres through the contacts before the gage circuits are triggered, and the compressive wave usually does not arrive at the gage location until from 10 to 20 μ s later. This time is important because the reference baseline from which strains are determined becomes more stable as the interface area between the probe and contact increases. A steel shield placed in front of the target surface protects the probes and wires from ejected particles. These experiments are conducted in a vacuum and conducting air shock is not a problem. However, at impact velocities above 950 m/s, conducting vaporous ejecta expands around the ejecta shield and can reduce the resistance between probes, producing a false signal which resembles compressive strain. Surface ejecta will be considered in more detail later when problem areas are discussed. False signals from conducting ejecta are prevented by insulating all conductors exposed on the target side of the probe support. Vaporous ejecta has also been an occasional problem when probes pierce the contacts on the sabot. Interaction between gages has been prevented by interposing

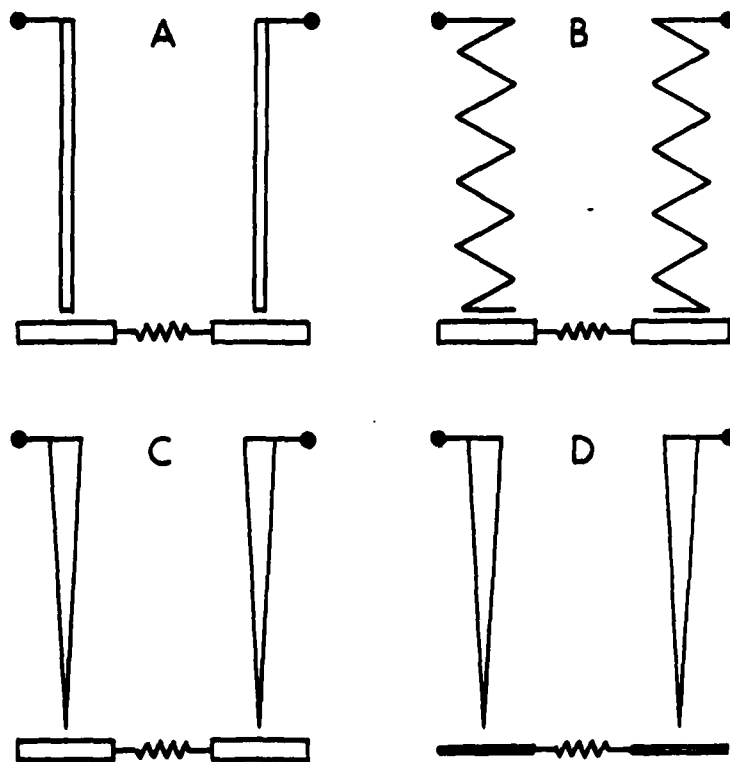
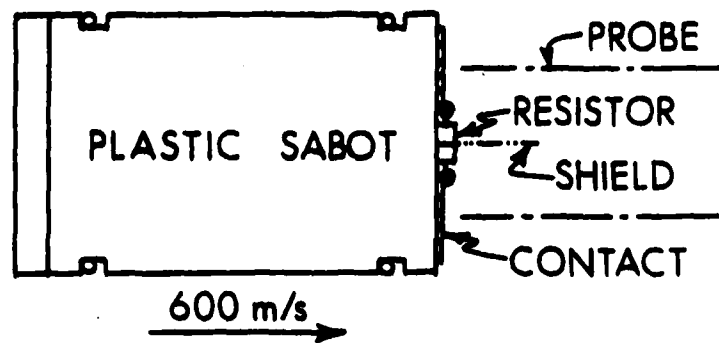


Figure 1. Configurations of probes and contacts tested to determine if a low-resistance electrical path could be maintained between stationary probes and contacts moving at ballistic velocity.

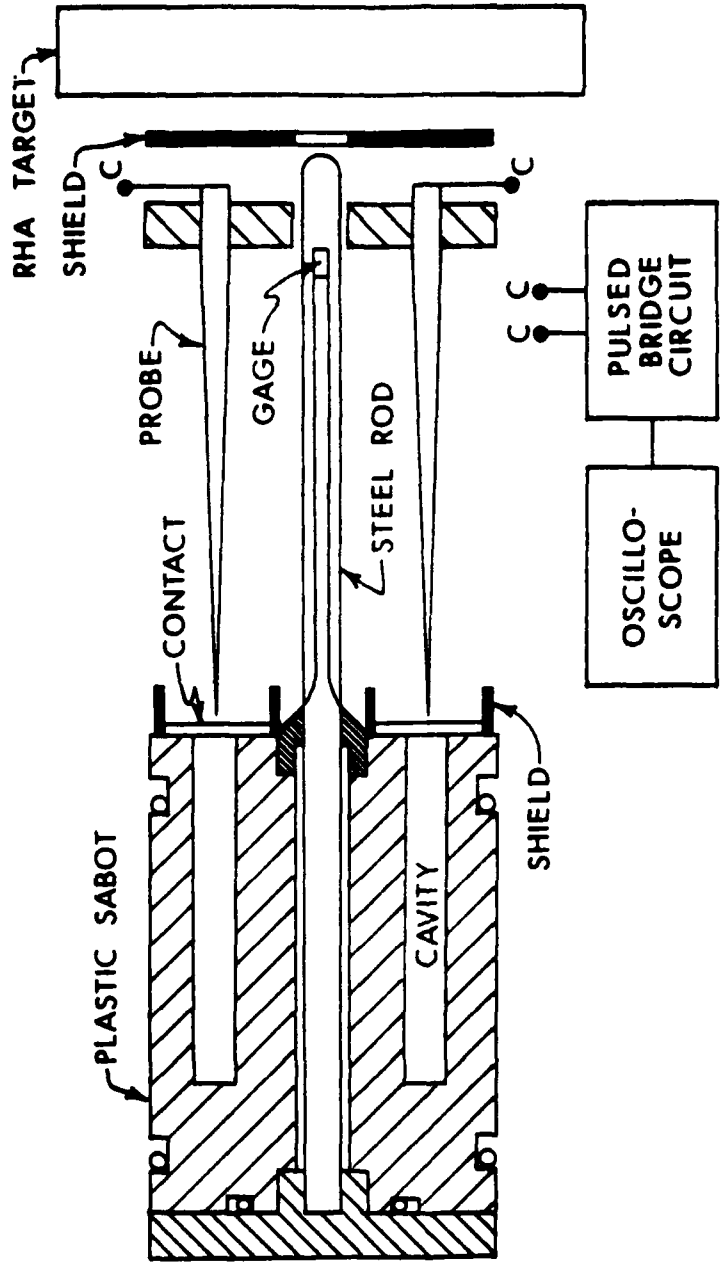


Figure 2. Experimental arrangement for forward-ballistic experiments.

shields and coating probe and contact surfaces with a thin film of plastic which insulates against vaporous conduction without affecting conduction between the probe and contact.

C. Strain Gages.

Type EP high-elongation foil gages manufactured by Micro-Measurements, Inc., were selected because this type of gage was used by Sharpe⁴ for impact studies with annealed aluminum in which he demonstrated close agreement with interferometric measurements of strain to eight percent. Although Sharpe reported accurate response for 1.57mm (0.062 inch) foil gages, he found that 6.35mm (0.250 inch) foil gages failed to respond correctly and indicated a maximum strain that was 20 percent low. In the instrumented rod measurements, gages were bonded to the steel rods with the M-Bond AE-15 epoxy system marketed by Micro-Measurements, Inc., and it was not known that this adhesive would provide the response reported by Sharpe. Consequently, a series of impact experiments was performed with 1.57mm and 3.18mm Type EP gages bonded to annealed aluminum with AE-15 epoxy. These tests were performed at The Johns Hopkins University and duplicated earlier experiments by Bell⁵ in which the strain was measured by ruled diffraction gratings. Strain measured by the 1.57mm gages was in agreement with strain measured by gratings, although strain measured by 3.18mm gages lagged the correct strain and reached a maximum value which was approximately 13 percent low. These results were in general agreement with results reported by Sharpe. When impact experiments were later performed with 1.57mm and 3.18mm gages at the same location on steel rods, the measured strains were closely comparable. These results indicate that the presence of a large gage reduces the strain in measurements on annealed aluminum, but has a negligible influence in measurements on hard steel. There has been interest in the 3.18mm gage because the manufacturer reports that the maximum elongation capability exceeds that of shorter gages. However, the ability of 3.18mm gages to measure compressive strains larger than those which can be measured by 1.57mm gages has not yet been fully investigated in impact experiments. It has been determined that the 1.57mm gage can respond to apparent compressive strain of 25 percent or more in impact experiments. Debonding has not been observed and the reason for signal loss is not always well established. Signal loss will be considered more fully in the later discussion of problem areas. Although gages respond to compressive strains apparently greater than 20 percent, the reliability of dynamic strain measurements above 8 percent has not yet been established. Reliability will be discussed later when problem areas are considered in more detail.

⁴W. N. Sharpe, Jr., "Dynamic Plastic Response of Foil Gages", *Experimental Mechanics*, Vol. 10, No. 10, October 1970, pp. 408-414.

⁵J. F. Bell, "Propagation of Large Amplitude Waves in Annealed Aluminum", *J. Applied Physics*, Vol. 31, No. 2, February 1960, pp. 277-282.

D. Strain-Gage Circuit.

Probes are connected to bridge circuits which are triggered after the contacts have been pierced. A circuit is shown schematically in Figure 3, and is essentially a bridge circuit of the type examined by Rice⁶. Each gage is connected (through the contacts and probes) to a circuit by ten metres of coaxial cable with a characteristic impedance of 125 ohms. A 5-ohm resistor in series with each 120-ohm gage initially provides the correct termination. Data have been recorded with oscilloscopes, and the coaxial signal cable has been terminated at the oscilloscope with its characteristic impedance of 185 ohms. With this choice of cables and bridge resistances, the gage and signal cables are correctly terminated in both directions. During a test the sabot and rod are loaded into the gun, and gages on the rod are not used for calibrations. Instead, oscilloscopes are calibrated with a substitute gage which is temporarily connected to the gage cable. Calibration consists of pulsing the gage with several values of parallel resistance; the results are used to evaluate constants in the circuit equation and establish a deflection factor. The correct resistances of gages on the rod are introduced for the determination of strain. Signals are usually divided and recorded by two oscilloscopes, one recording 0 to 5 percent strain, and the other 0 to 25 percent strain. The circuit was designed to operate below the threshold of apparent strain for gages with a length of 1.57mm. Calculations supported by heating tests on pulsed temperature sensors indicate a temperature increase of less than 50°C for a pulse duration of 100 μs. During calibration switch S2 is usually closed after 70 μs to divert current from the gage cable and reduce the danger of damaging the gage by overheating. The use of a substitute gage for calibration eliminates the possibility of destroying a gage on the rod if S2 does not function.

E. Sabot Orientation.

The forward-ballistic technique requires each probe to be correctly oriented with respect to the corresponding contact. During launch, the sabot must maintain the correct orientation with which it was loaded in the breech. Rotation has not been a common problem of projectiles launched from the 100mm light-gas gun which is used for these tests. When rotation has occurred, it has apparently been associated with the use of an unbalanced projectile. When unbalance cannot be avoided, the projectile is loaded in the orientation it naturally assumes on a horizontal surface plate.

III. REVERSE-BALLISTIC TECHNIQUE

Reverse ballistics refers to the experimental approach in which targets are launched at stationary projectiles. A reverse-Ballistic

⁶M. H. Rice, "Calibration of the Power Supply for Manganin Pressure Gages", Air Force Weapons Laboratory Technical Report No. AFWL-TR-70-120, November 1970.

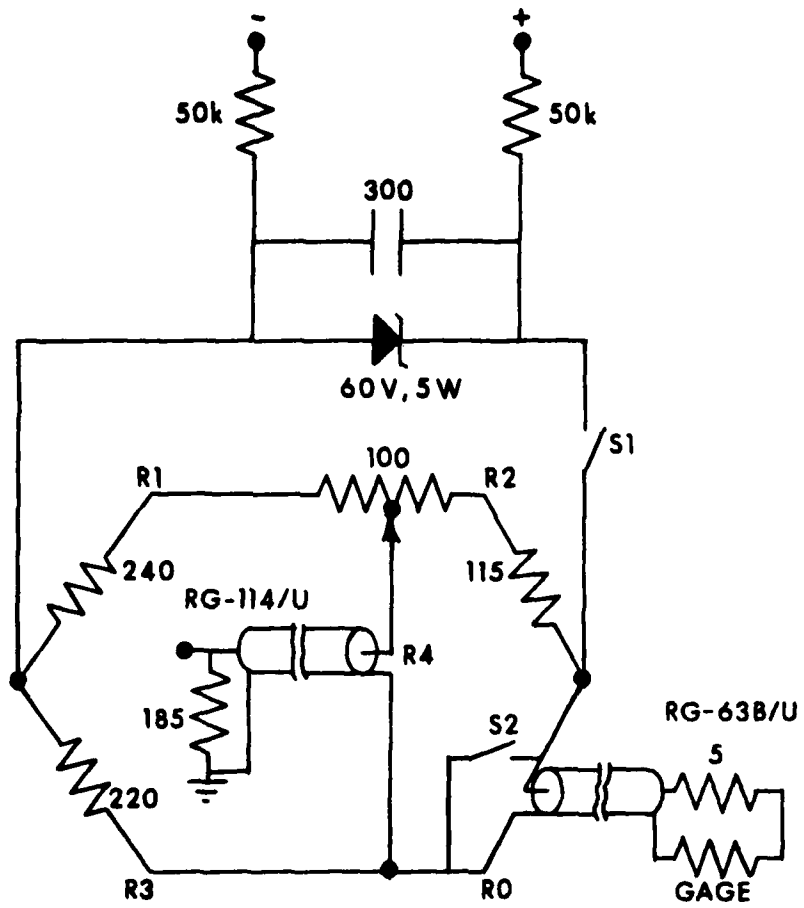


Figure 3. Bridge circuit for strain-gage measurements.

experiment with an instrumented long-rod penetrator is shown schematically in Figure 4. Reverse-ballistic experiments have been performed at the BRL using a light-gas gun with a bore of 100mm and a length of 14m. This bore imposes a restriction on the target diameter. Furthermore, this gun is operated in the laboratory and the target and penetrator must be retained in a catcher. The energy limitation of the catcher imposes a restriction on either the target mass or the impact velocity. Despite the limitations of reverse ballistics, it nevertheless offers some important advantages. The strain-gage signals are usually superior to those from forward-ballistic experiments, and signal quality is a major consideration in analyses. Reverse ballistics also does not impose a limitation on the number of gages, and analyses benefit from data of more than three gage pairs. Reverse ballistics also permits experiments with longer rods and longer recording times, and this allows the slowly-moving high strain levels to be recorded at widely spaced rod locations. The forward-ballistic configuration in Figure 2 does not permit observation times longer than 70 or 75 μ s at an impact velocity of 1000 m/s. Finally, reverse ballistics provides a situation in which penetrator displacement results only from particle motion associated with the stress waves; without large displacements associated with the impact velocity, other measurement techniques are more accurately employed to provide data which can be compared with strain-gage results.

The sections on strain gages and the strain-gage circuit, which were included under forward ballistics, also apply to the reverse-ballistic technique. Constant gage excitation prior to a penetration experiment could be used in reverse ballistics, but pulsed operation permits the use of higher excitation currents and provides larger signals for an improved signal-to-noise ratio.

IV. DISCUSSION OF PROBLEM AREAS AND RESULTS

A number of problem areas have been encountered during experiments with instrumented long-rod penetrators. Before useful data were obtained, problems from target ejecta had to be solved. When useful strain/time results were obtained, records were frequently found to end at low strains and the reasons for premature loss of signal were explored. Records were commonly troubled by noise and distortion, and sources of these troubles were examined. The number of strain gages used to instrument a penetrator became an important consideration in the analysis of data, and further influenced the choice of measurement techniques. Data reduction has presented problems, and procedures have been modified frequently in efforts to achieve greater accuracy. Finally, the reliability of data and analyses has needed verification; although there has been progress in this area, further study is needed. Each of these areas will be considered in this section of the report.

A. Target Ejecta.

Trouble from electrically conducting target ejecta was encountered during development of the forward-ballistic technique. Consequently, impact and penetration were examined photographically to determine the nature of target ejecta. Figure 5 shows selected photographs from the framing camera record of an experiment in which a steel rod, launched at 1000 m/s, penetrated a 25mm thick target of rolled homogeneous armor. Time, relative to impact, is shown in the lower right corner of each photograph of the sequence. Immediately after impact, a high-velocity steel jet is produced as the hemispherical tip of the rod encounters the plane target surface. The leading portion of this jet is composed of conducting vapor which produced a false signal when it arrived at the probes which were uninsulated in early forward-ballistic experiments. The vaporous portion is followed by small particles which also move away from the impact area at a wide angle. The vaporous ejecta quickly dissipates, and as it does, the slower moving massive ejecta becomes evident. Fragments of the slower ejecta which can be identified in successive photographs indicate motion directed away from the rod at a narrow angle and this suggests that gages could be carried for some distance into the hollow column of slow ejecta without being destroyed. It was anticipated that an ejecta shield would be effective for confining the vapor and small particles which move away from the rod at a wide angle. Shields were included in the experimental arrangement for forward ballistics where they were not highly effective in suppressing false signals. However, shields were later used effectively to confine the vaporous ejecta in reverse ballistic experiments, providing clear optical observations of detail on the surface of the rod.

Jetting is undoubtedly influenced by the configuration of the rod tip. A hemispherical tip was used initially because this was the common configuration. Although the tip configuration has not received much consideration in the instrumented rod investigation, the hemispherical tip has been found to be preferable to a flat end because it tends to suppress Pochhammer-Chree oscillations.

B. Signal Loss.

Strain/time records frequently end while gages are still at low strain levels. Signal loss is a concern in both forward-ballistic and reverse-ballistic experiments. The premature end of a strain record implies either shorting or loss of electrical continuity; debonding of a gage has never been clearly identified in instrumented penetrator experiments. Signal loss is believed to result from damage to either the lead-wire or the gage.

In the experimental arrangement for forward ballistics, shown in Figure 2, leadwires are especially vulnerable at the location where they cross from the rod to contacts on the sabot. After impact, particle velocity associated with the compressional wave in the rod produces

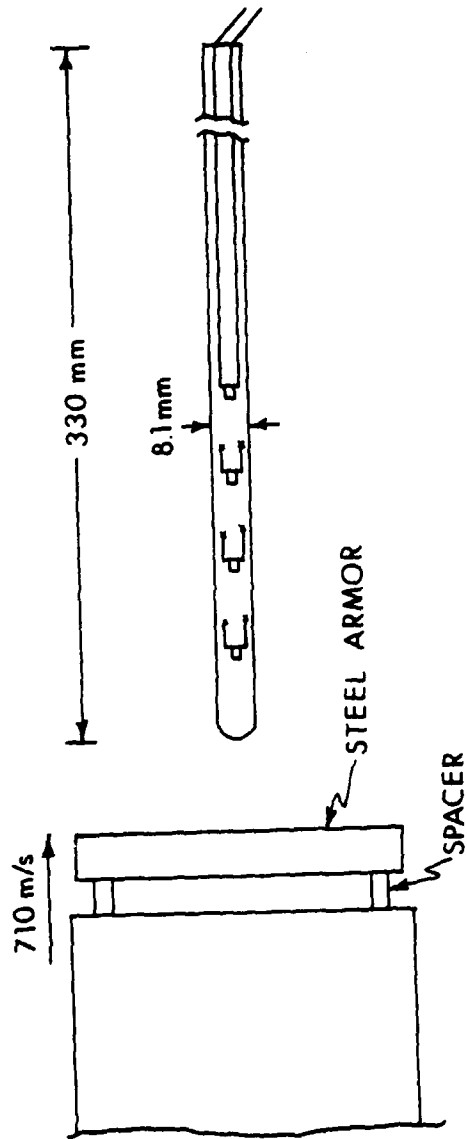


Figure 4. Experimental arrangement for reverse-ballistic experiments.

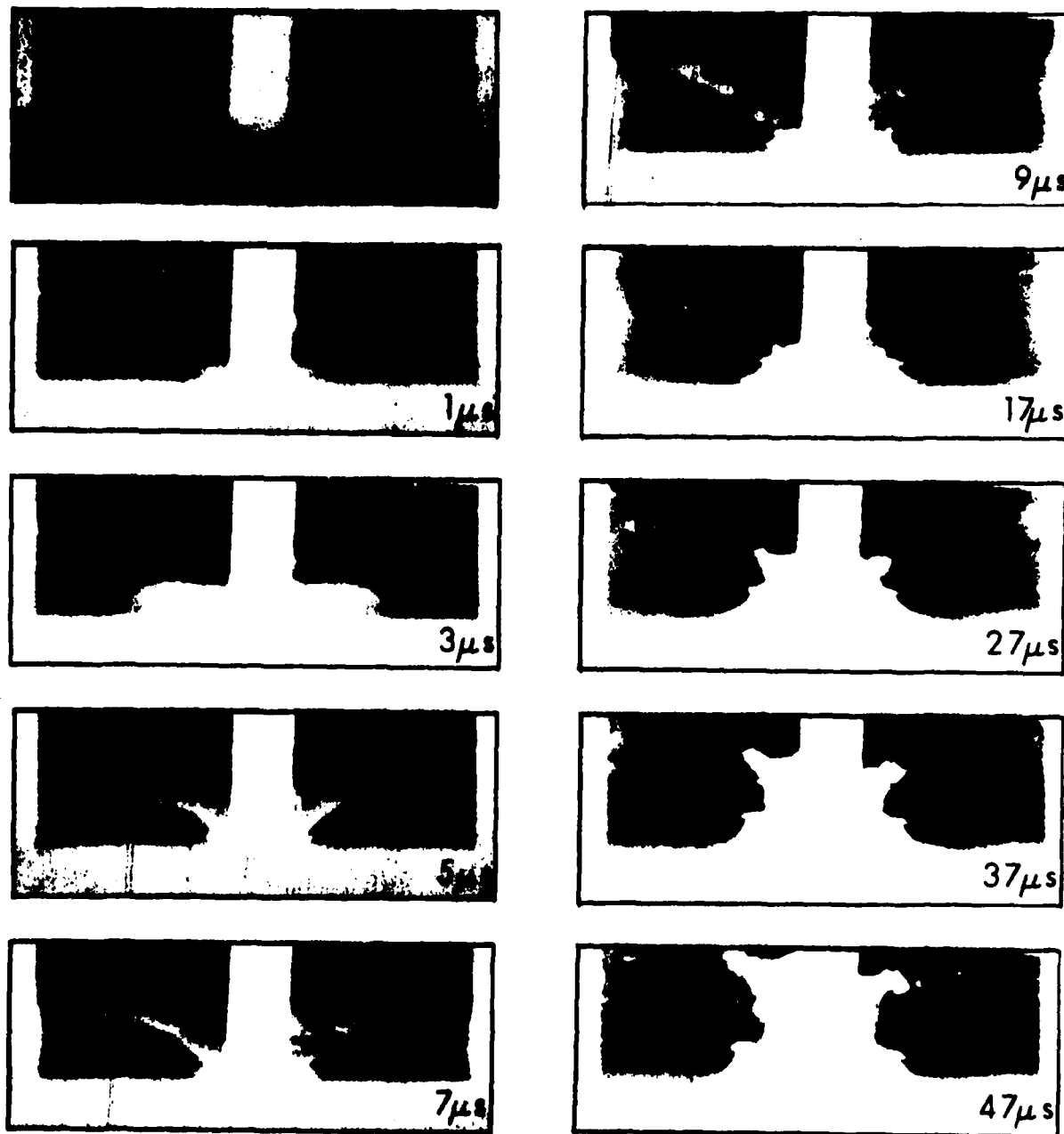


Figure 5. Photographic study of target ejecta produced when a long steel rod strikes steel armor at a velocity of 1000 m/s.

deceleration, and the rod is gradually displaced from the sabot which continues at the impact velocity. If single-conductor leadwires of AWG-34 copper are rigidly secured to the rod and sabot near the cross-over point, the gage signal is lost quickly. If these leadwires continue to the back of the rod and return through the sabot to contacts on the surface, signal loss is delayed; the amount of delay depends upon the configuration at the back end of the rod. The most successful leadwire for forward ballistics has been vinyl-insulated AWG-26 stranded copper, secured to the rod and sabot by minimal fillets of Hysol 608 epoxy. This configuration produced the strain/time records shown in Figure 6. These records are from a forward-ballistic test in which an instrumented steel rod impacted a 25mm thick RHA target at a velocity of 1000 m/s. At 20mm and 40mm from the tip of the rod, signals continued to the limit of observation at strain of 0.150 (15 percent). At 60mm, the record ended at strain of 0.064 (6.4 percent). These data were combined with data from an identical experiment, and a simple-wave analysis was performed to obtain the stress/strain and particle velocity/strain relationships shown in Figure 7. Strain/time records were then converted to particle velocity/time and integrated to provide the displacement/time curves shown in Figure 8. Figure 8 suggests that signal loss occurred when displacement between the rod and sabot was approximately 1.5mm. Although a displacement of 1.5mm at the cross-over point might break the AWG-26 leadwire, further consideration is appropriate.

Displacement/time results were also used to construct a time/distance diagram in laboratory coordinates. This diagram appears in Figure 9 and includes paths for the elastic wave in the rod and the fast and slow target ejecta. The diagram suggests that gages are destroyed as they arrive at the target surface. Strain/time records from a reverse-ballistic experiment at a lower impact velocity were also analyzed to find where signal loss occurred. These strain/time records, shown in Figure 10, are superior to the records shown in Figure 6. Stress-strain and particle velocity/strain results from a simple-wave analysis of these records are shown in Figure 11. Following the same procedure, a time/distance diagram was constructed in laboratory coordinates and is shown in Figure 12. This diagram also suggests that gages are destroyed close to the target surface, in fact, closer than suggested by the gage paths at 20 and 40mm. These paths end at the onset of bending. If continued to where signal loss actually occurred, the 20mm gage survives to within 1.5mm of the surface and the 40mm gage survives to within 1.0mm. The gage at 80mm was still intact at the end of the recording interval and there is no estimate of where signal loss occurred.

The forward-ballistic test at 1000m/s and the reverse-ballistic test at 710 m/s both indicate that signals end when gages arrive at the target surface. When measurements to high strain are an important consideration, reverse-ballistic tests are performed using a target with a reduced diameter which permits eroded rod and target material to move away from the rod. With a target diameter/rod diameter ratio of 3.0, gages at 20, 40, and 60mm from the tip of the rod have recorded apparent

strains of 0.25 (25%) or higher in an experiment at 1000 m/s. A ratio of 4.0 caused premature loss of signal, while a ratio of 1.6 apparently provided an unstable forcing function and produced erratic strain/time records.

Signal loss apparently occurs for different reasons. Leadwires can fail during the displacement that occurs after impact. However, if leadwires are properly selected and supported, they survive the displacement and signal loss eventually results from gage destruction. With a semi-infinite target, gages are destroyed by ejecta as they arrive at the target surface. However, if the target diameter can be reduced, eroded material moves away from the rod and strain-time measurements can be continued into the target.

C. Signal Distortion and Electrical Noise

Signal distortion has been encountered only in forward-ballistic measurements. The record at 60mm in Figure 6 is distorted, and this distortion is believed to have resulted when the rod was perturbed by sabot material displaced by the probes. This type of distortion was not observed after cavities were introduced beneath each contact on the sabot surface. Distortion is also produced by variations in resistance that are not related to the strain. Some variations in resistance can be attributed to the probes and contacts, especially at early times after the contact is pierced when the interface area is small. Such distortion precedes the signal in Figure 13-A. As the interface area increases with time, the resistance becomes less variable. The basic problem is actually related to the time available for measurements. Probe lengths have been 100mm, and at an impact velocity of 1000 m/s, this length permits a maximum recording time of 100 μ s; at higher impact velocities, the maximum recording time is even less. After allowing time for circuits to stabilize and for probe-contact resistance to diminish, 70 μ s or less remains for the strain-gage signal, and this is only enough time for a 20 percent strain level to travel approximately 50mm in a steel rod. In principle, probes could be lengthed for measurements further from the tip of a rod, but the sabot would have to be redesigned to eliminate the aluminum base plate which would be contacted by longer probes.

Signal noise arises from different sources, and is undesirable because it reduces the accuracy of test data. Figure 13-A shows noise which is attributed to vinyl insulation on leadwire used in forward-ballistic tests. When vinyl-insulated wire was replaced by polyimide-insulated wire, signal quality improved. Single-conductor AWG-34 copper wire insulated with polyimide film was used in reverse-ballistic tests to obtain the records shown in Figures 13-B and 13-C. Bursts of noise along an otherwise noise-free signal are produced when forward strain gages are destroyed. The most degrading noise is that shown in Figure 13-D. This signal is noise free until the first gage is destroyed; noise is then continuous and severe. Crowbarring the destroyed gages had no influence on this noise. Epoxy which secured leadwires to the rod was suspected

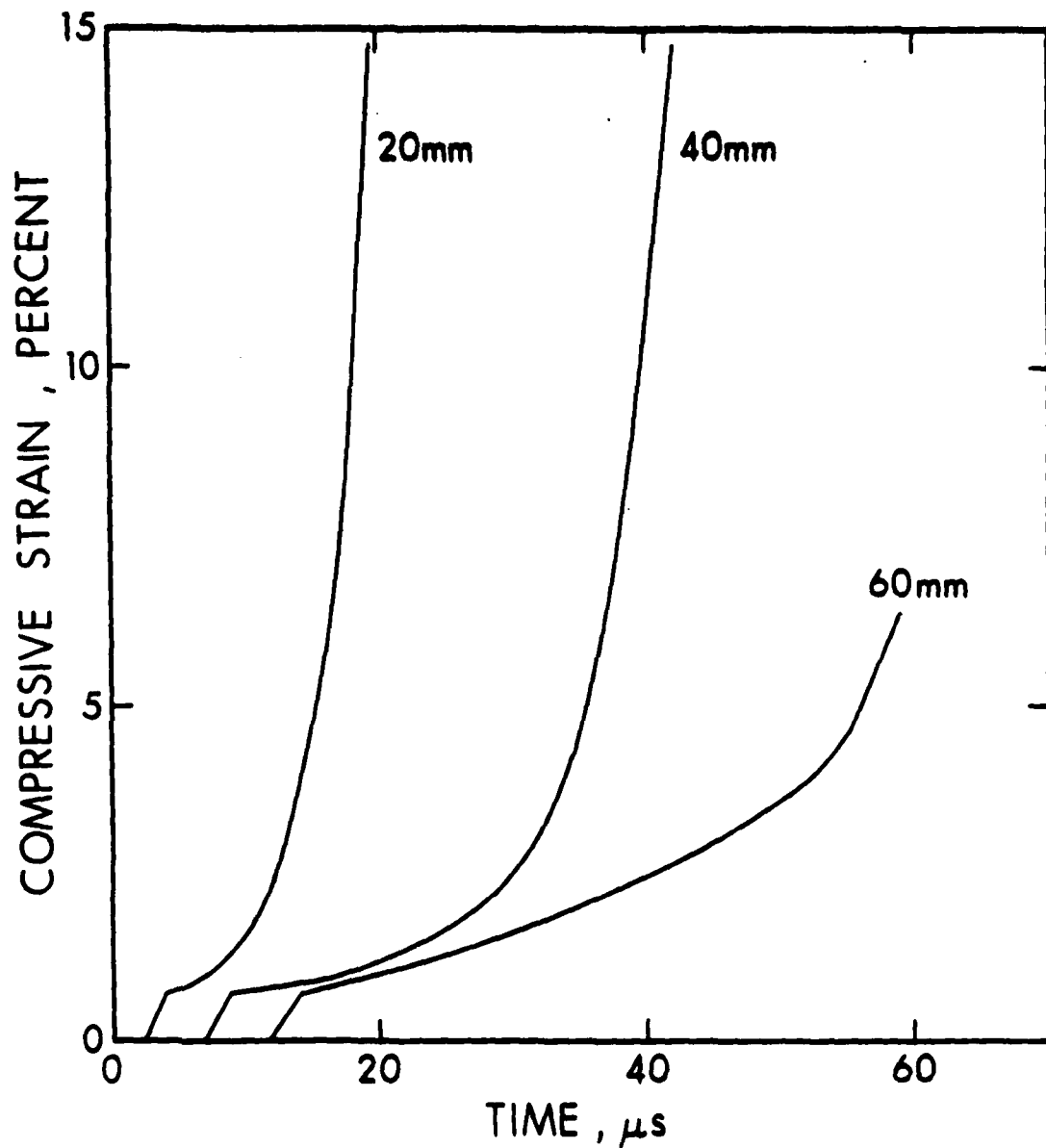


Figure 6. Strain/time records from an early forward-ballistic experiment with strain gages located 20, 40, and 60mm from the tip of the rod.

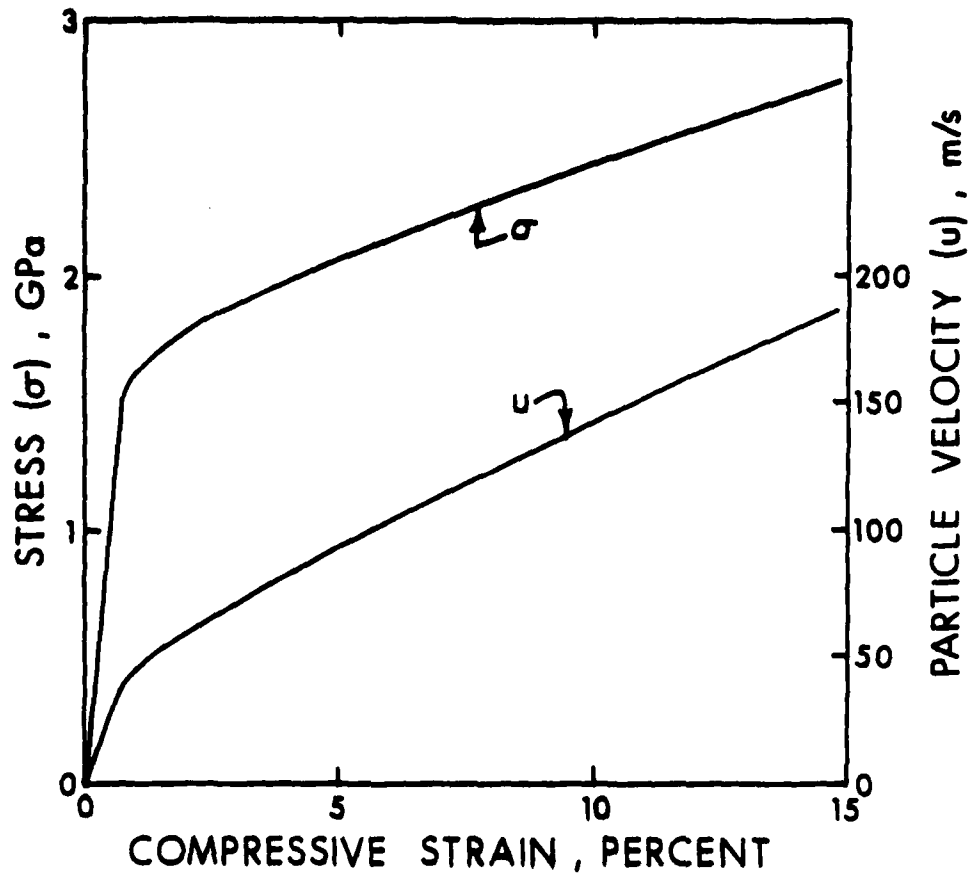


Figure 7. Stress/strain and particle velocity/strain relationships obtained by a simple-wave analysis of strain/time records which included those shown in Figure 6.

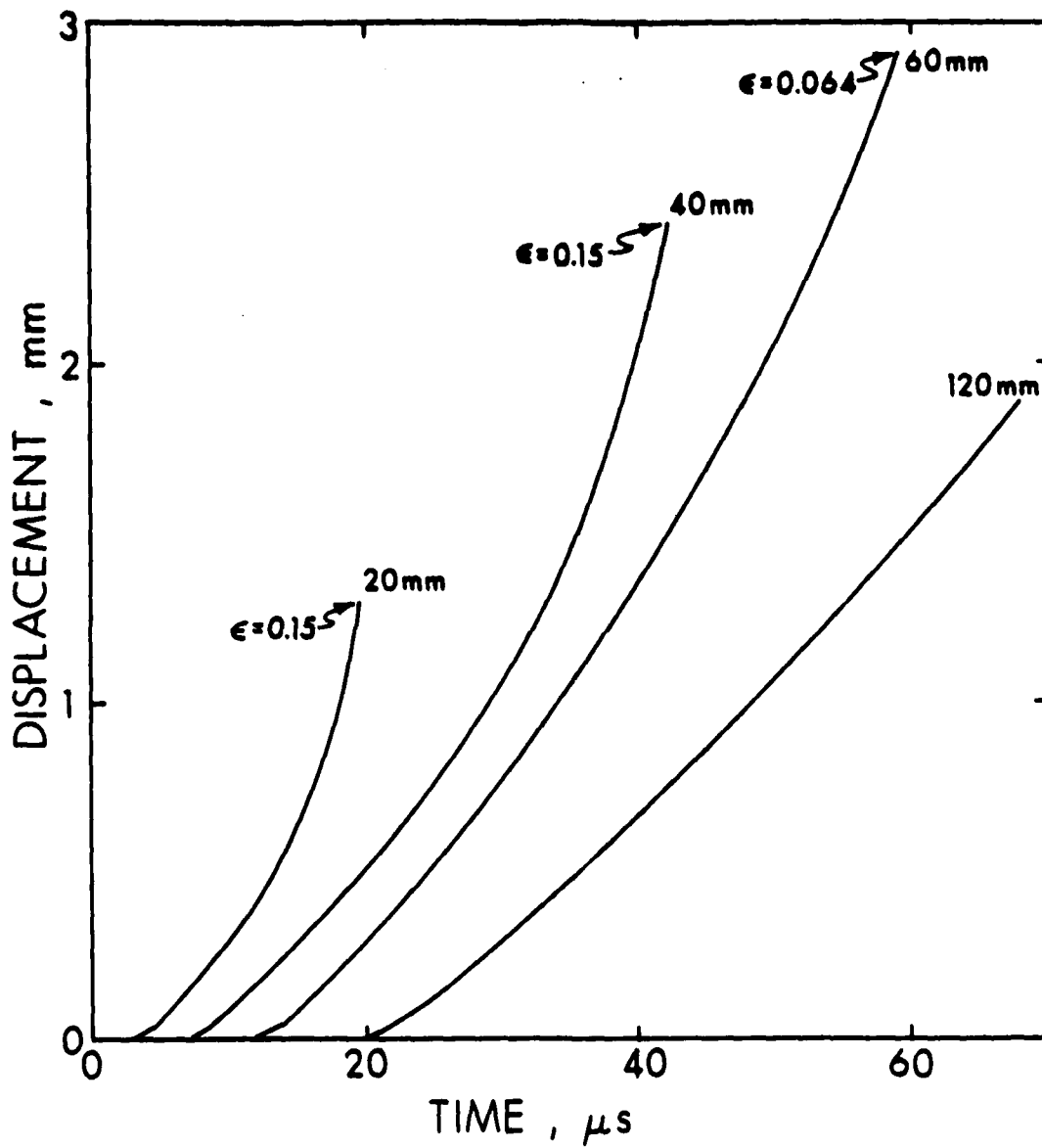


Figure 8. Displacements, relative to the sabot, that occur when the steel rod deaccelerates after impact in the forward-ballistic experiment at 1000 m/s.

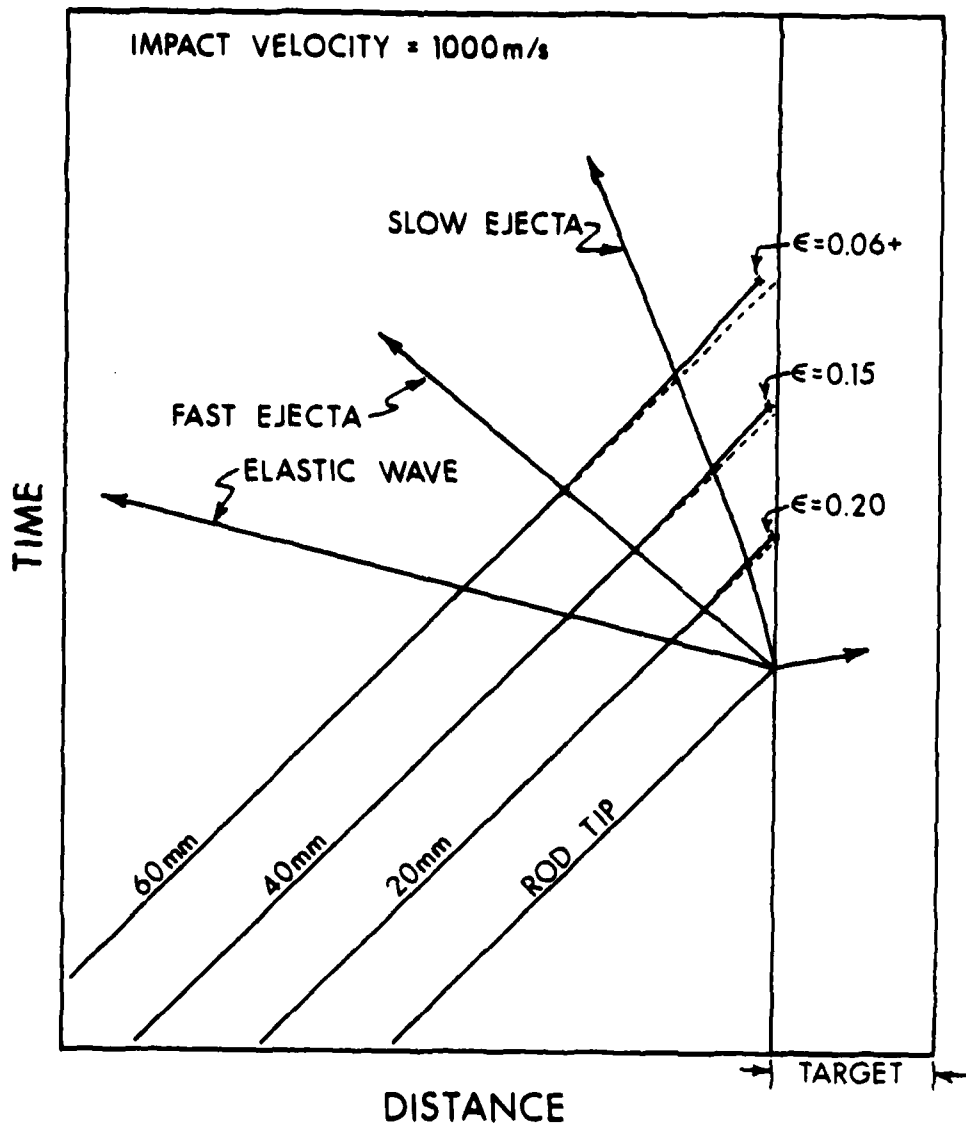


Figure 9. Time/distance diagram in laboratory coordinates, showing a steel rod impacting a steel target at 1000 m/s.

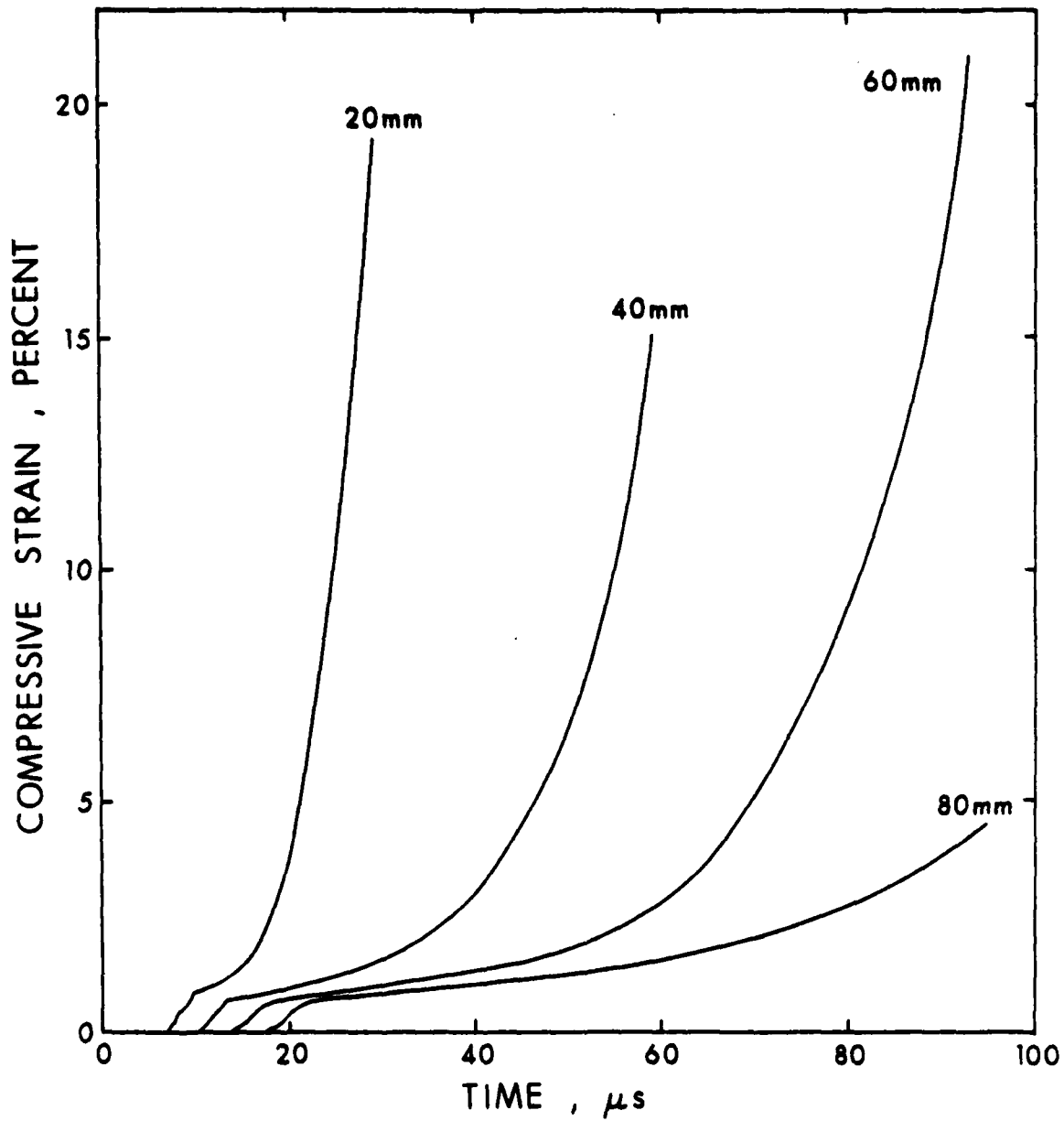


Figure 10. Strain/time records from a reverse-ballistic experiment in which a stationary steel rod was impacted by a steel target launched at 710 m/s.

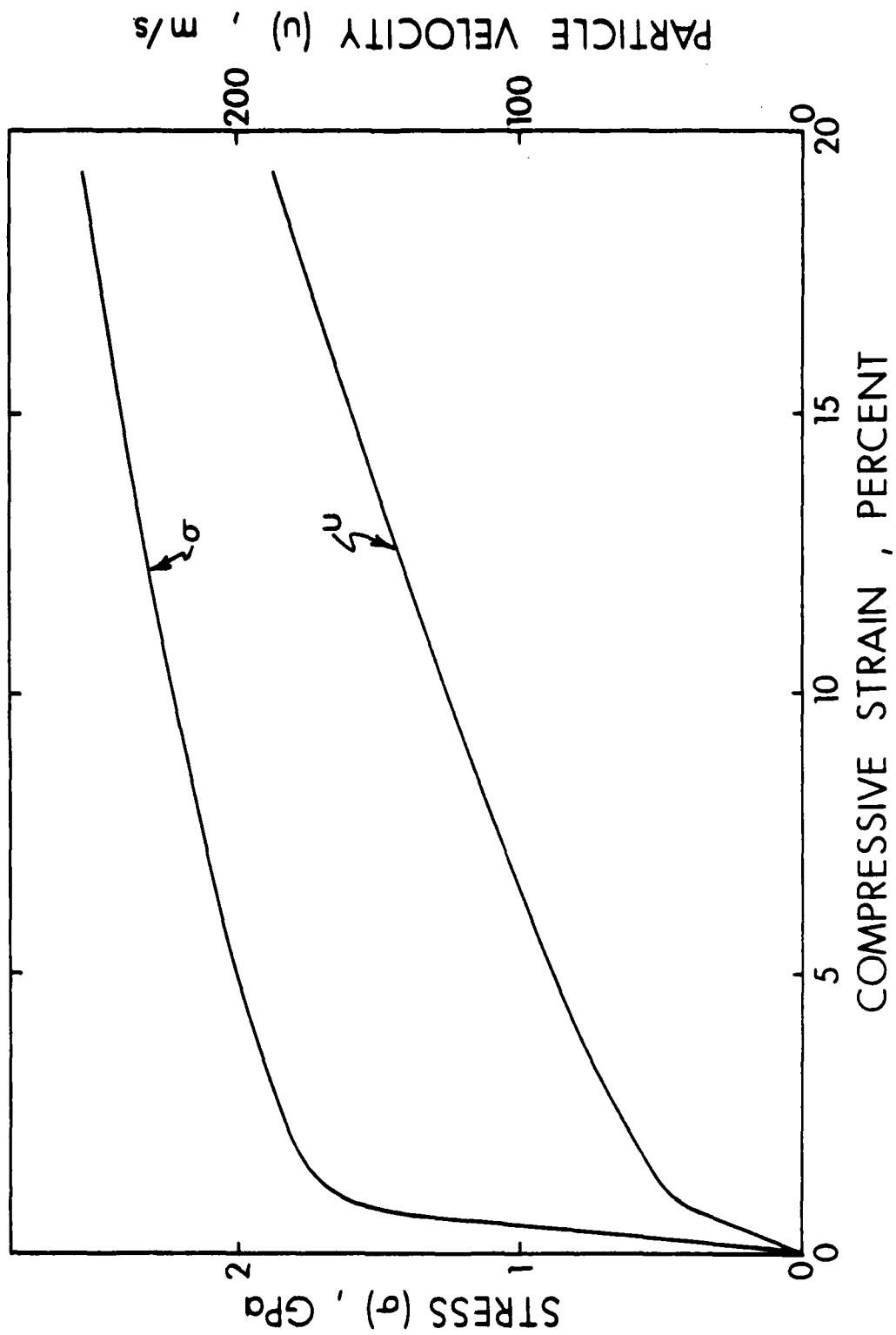


Figure 11. Stress/strain and particle velocity/strain relationships obtained by a simple-wave analysis of the strain/time records shown in Figure 10. 25

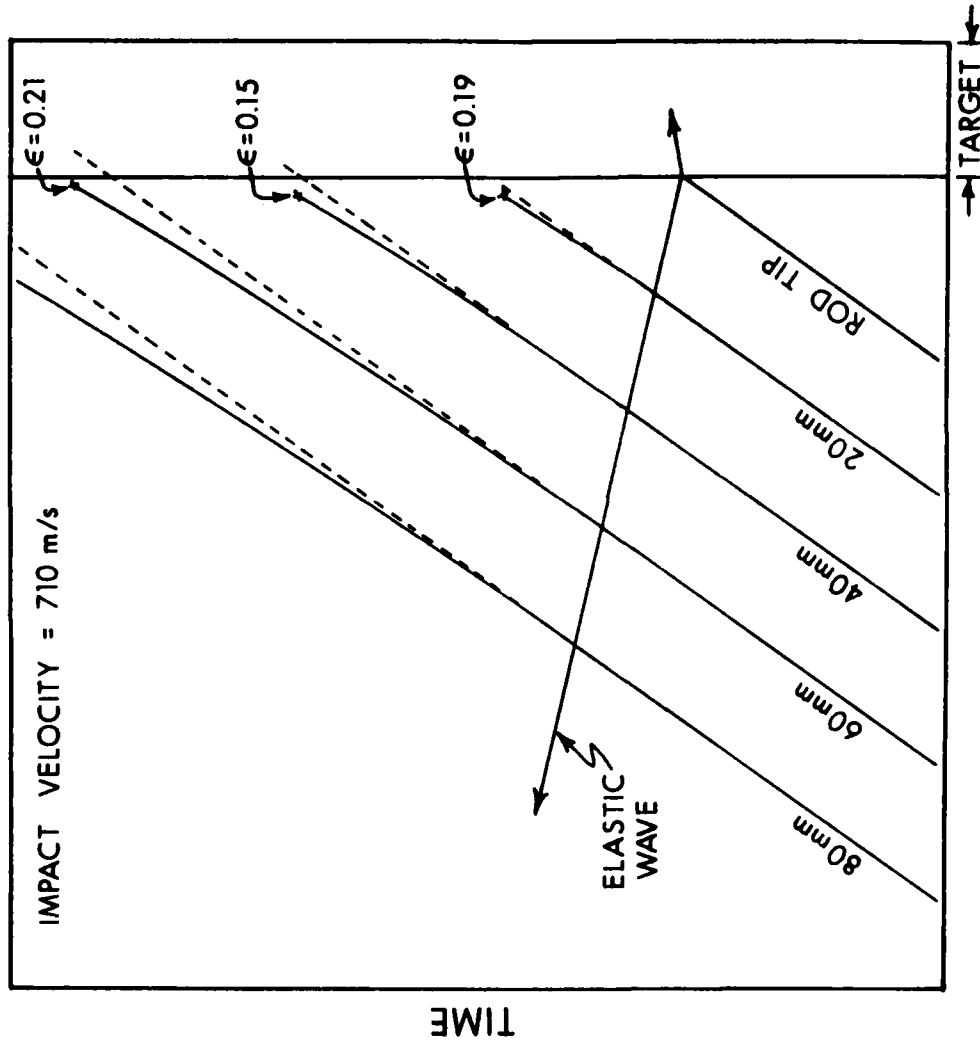


Figure 12. Time/distance diagram in laboratory coordinates, showing a steel rod impacting a steel target at 710 m/s.

but was found not to be a contributor. Residual magnetism was also suspected. In reverse-ballistic tests, gages on the rod are pulsed to rebalance the bridge circuits after calibration; an increase in magnetism is found after the eight or ten gages have been pulsed. Rods were given a final demagnetization before the test even though noise-free signals were previously obtained with steel rods without following this procedure. Despite the final demagnetization, noise persisted. The noise was traced to a single lot of rods, although all lots were prepared from the same source of VIMVAR processed tool steel and should have received identical heat treatments. The behavior of this single lot of rods has not been explained.

Noninductive strain gages have been considered for rod locations where noise levels tend to be higher, but have not been tested to learn if induced noise is suppressed. Noninductive gages have been prepared and at low strain levels their response agrees closely with the response of single gages; agreement at high strain levels has not been tested. These noninductive gages were fabricated from high-elongation strain gages, bonded in register using AE-15 epoxy. The overlaid gage was partially etched away, and rebuilt with electroplated copper to provide a total resistance only slightly more than 120 ohms. The registered gage elements were then opposed in series with the overlay acting essentially as an antenna. Data have been reduced by applying a gage factor of $(2+\epsilon)$ to the total resistance of the noninductive combination. Investigations with noninductive gages were not actively pursued after it became apparent that the most degrading source of signal noise could be avoided by heat treating procedures.

D. Number of Gages

The number of gages used in each experiment has increased as instrumented rod investigations have progressed; the additional data have been helpful in analyses. Early forward-ballistic experiments employed four gages, but the number was soon increased to six, providing diametrically opposed pairs at three locations on the rod. The six gages required seven probes and contacts, with one contact common to all gages. Confidence in sabot alignment during the launch did not justify the use of additional gages, and this has been a major limitation of the forward-ballistic technique. From eight to ten gages are commonly used in reverse-ballistic experiments, and signals from the three or four pairs of forward gages are divided and recorded at different deflection sensitivities for improved resolution. (Unloading at the back end of the rod prevents the back gages from experiencing high strains.) Gages are usually arranged in diametrically opposed pairs; this practice is followed because bending is more common than suggested by the early penetration experiments with instrumented rods. Bending is evident in the oscilloscope records shown in B and E of Figure 13.

E. Data Reduction

Signals from strain gages on instrumented penetrators are reduced to obtain strain and time. Strain, ϵ , is determined by the relationship,

$$\epsilon = x/g,$$

where x includes the gage resistance and resistance change, and g is the gage factor. The gage factor for high elongation gages is assumed to be $(2+\epsilon)$, and this assumption is supported by quasi-static tests by Franz⁷ who compared optical and foil-gage measurements to strain of 0.16 (16 percent). The term, x , is given by

$$x = \left[(C_1 D_t) / FR_g \right] / \left[1 - D_t (C_2 / F) \right],$$

where D_t is the measured signal displacement. C_1 and C_2 are circuit constants, where

$$C_1 = (R_o + R_3) \left[1 + R_o(R_3 + R_4) / R_3 R_4 + R_o(R_1 + R_2) / R_4(R_o + R_3) \right],$$

and

$$C_2 = \left[(R_o + R_3)(R_3 + R_4) / R_3 R_4 \right] + R_o(R_1 + R_2) / R_4(R_o + R_3).$$

Resistances R_o , R_1 , R_2 , R_3 , and R_4 are identified on the circuit diagram in Figure 3. The deflection factor, F , is determined by calibrations. Calibration consists of introducing parallel resistances, R_c , to produce resistance changes, $\Delta R'$; depending upon the strain range of the record, calibrations correspond to strains of 0.01, 0.02, and 0.05, or 0.05, 0.10, and 0.20. F is determined from the relationship,

$$F = D_c \left[(C_1' + C_2' \Delta R') / \Delta R' \right],$$

where D_c is displacement measured on the calibration record, C_1' and C_2' are the circuit constants, and $\Delta R'$ is determined by the usual expression

$$\Delta R' = R_g' \left[R_c / (R_c + R_g') - 1 \right].$$

Primed values refer specifically to the calibration, with R_g' being the resistance of the gage used for all calibrations, and C_1' and C_2' based on

⁷R. E. Franz, "Volume Changes in Metal Alloys Due to Plastic Deformation", Ballistic Research Laboratory Memorandum Report (In Preparation).

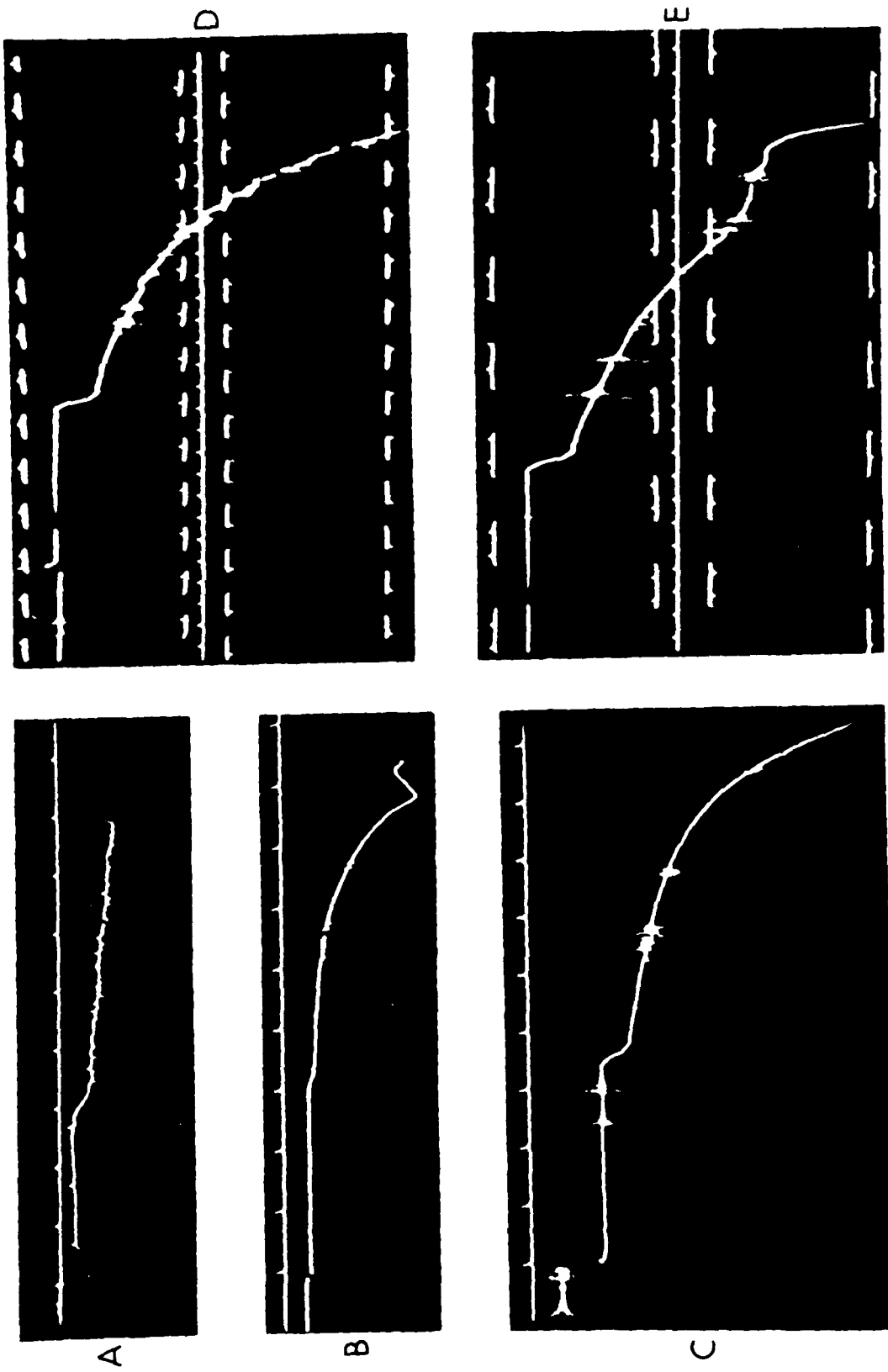


Figure 13. Oscilloscope records.

primed values R'_0 , R'_1 , and R'_2 . Data are presently reduced using the mean value of F based on a calibration with three values of R_c .

Oscilloscopes have been used to record strain-gage signals. The photographic records of these signals are slightly distorted, and this distortion can complicate record reduction and degrade the accuracy of results. The CRT display and the photographic film undoubtedly contribute to the distortion, but their contribution is not easily isolated from that of the recording camera which is believed to be the major contributor of positive distortion. Camera records are frequently photographed on Polaroid Type 410 film. If these records are copied to produce a transparency, additional positive distortion is introduced.

Small differences in the deflection factor, F , can usually be attributed to the influence of distortion. However, distortion is not being considered in the present determination of strain. Distortion is presently considered only in the determination of time. In the experiments with steel rods, the velocity of higher strain levels may approach one-eighth of the elastic-wave velocity, and total recording times of 150 μ s must be used to record some complete records. At this record duration, 0.025mm (0.001 inch) on the record may represent 0.1 μ s. Without corrections, timing errors of one microsecond or more can occur either directly from the distortion or from record misalignment which results from the presence of distortion. An example of record distortion is shown in Figure 14, and probably represents a combination of lens distortion and a secondary influence by mechanical instability of the recording camera. The square grid corresponds to the undistorted area which would be occupied by the signal or calibration. Image distortion is exaggerated in Figure 14 by using a magnification factor of 31.5 to plot the displacement of grid corners. The lower right corner of the distorted grid, for example, represents an actual horizontal displacement of +0.111mm (+0.0044 inch).

The procedure for treating distortion in the determination of time can be explained by reference to the strain-gage record shown in Figure 15. A reference sweep, located centrally where the influence of distortion is minimal, is provided for record alignment. Timing marks are superimposed on a square wave which is recorded twice, once above the reference line and once below the reference line, bracketing the total record. Time marks identified as line T2 serve as a reference, and time marks along line T3 are assumed to be displaced by a constant time difference. All time/distance relationships (T1, T2, T3, and T4) are represented by cubic fits. Time corrections, TC1, are required along T1, and time corrections, TC4, are required along T4. These corrections are also expressed by cubic fits, and the correction is assumed to vary linearly from T2 to T1 and from T3 to T4. No correction is used in the region between T2 and T3.

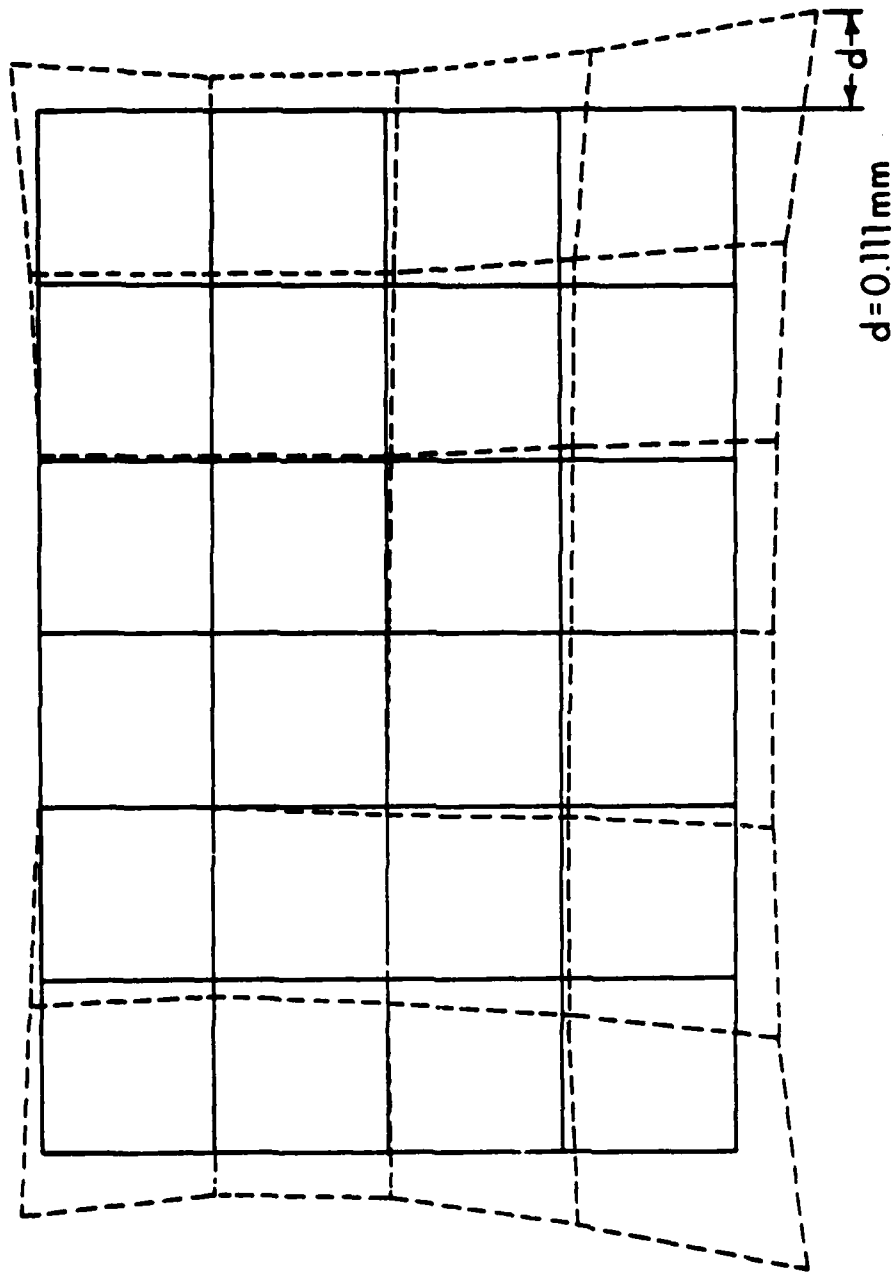


Figure 14. Typical distortion in an oscilloscope record.

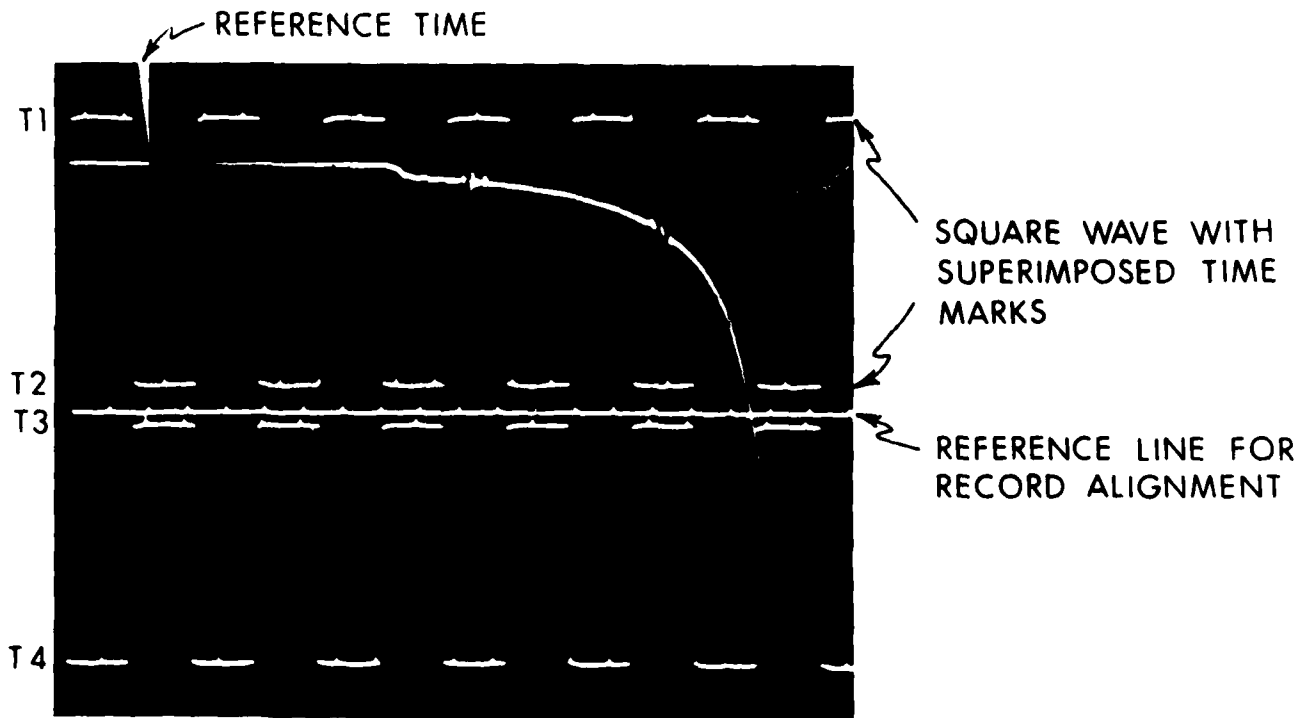


Figure 15. Oscilloscope record with features of the time calibration identified.

F. Reliability of Data and Analysis

As indicated previously, measurements by Sharpe and similar measurements during the present investigation have supported the reliability of high-elongation foil strain gages in dynamic measurements of strain below 0.08. Tests have also been performed to assess the reliability of both the gage measurements and the simple-wave analysis by which data have been treated. The particle velocity/strain relationship shown in Figure 4 was used to convert the strain/time signals in Figure 10 to particle velocity/time. Integration then provided displacement/time. Optical experiments were then undertaken to measure displacement/time for comparison. The experimental arrangement for optical measurements is shown in Figure 16 and is similar to the experimental arrangement for strain-gage measurements shown in Figure 4. However, an ejecta shield has been added to confine the target ejecta which can partially obscure detail on the rod surface. The steel rod was chemically darkened by gun bluing and an airbrasive unit was used to lightly abrade diffusely reflecting lines at 40, 60, and 80mm. These lines were then coated with aluminum by vacuum evaporation. The lines were illuminated by a Cordin High-Intensity Xenon Flash Unit and photographed by a Beckman and Whitley Model 339 Streak Camera as the rod was impacted by a target of rolled homogeneous armor launched at a velocity of 710 m/s. A representative displacement/time record is shown in Figure 16, and the actual photographic record is shown in Figure 17. Displacement begins with arrival of the elastic wave and each line is observed continuously until it is finally obscured by arrival of the ejecta shield. Figure 18 shows the comparison obtained at the 40mm location. The dots represent data from the optical measurement of displacement, and the solid curve represents displacement based on the simple-wave analysis of strain data. Essentially exact agreement is obtained to strain of 0.068 (6.8 percent) where the rod is obscured by the ejecta shield. As a test of sensitivity, the simple-wave analysis was repeated assuming that measured strains were five percent low. As shown by the dashed curve in Figure 18, assuming a five percent error shifts the curve well out of agreement with the optical results.

The highest strain level, 0.068, was obtained at the 40mm location on the rod. Since gages measure to apparent strain of 0.25 or higher, it is desirable to assess the reliability of measurements and analysis well above the 0.068 strain limit of the test described. It was estimated that a lower impact velocity of 450 m/s would permit observation to strain of 0.20 without obscuration by the ejecta shield. It is important not to encounter bending because optical and strain data are then more difficult to compare; a gage cannot be placed where the rod is observed optically and it is commonly located at a position diametrically opposed to the observed line. Preliminary results have indicated that the time to bending increases as the impact velocity decreases. Therefore, it was anticipated that bending should be less of a problem at 450 m/s than at 710 m/s.

An experiment was performed at 450 m/s, again employing the experimental arrangement shown in Figure 16. The photographic record from

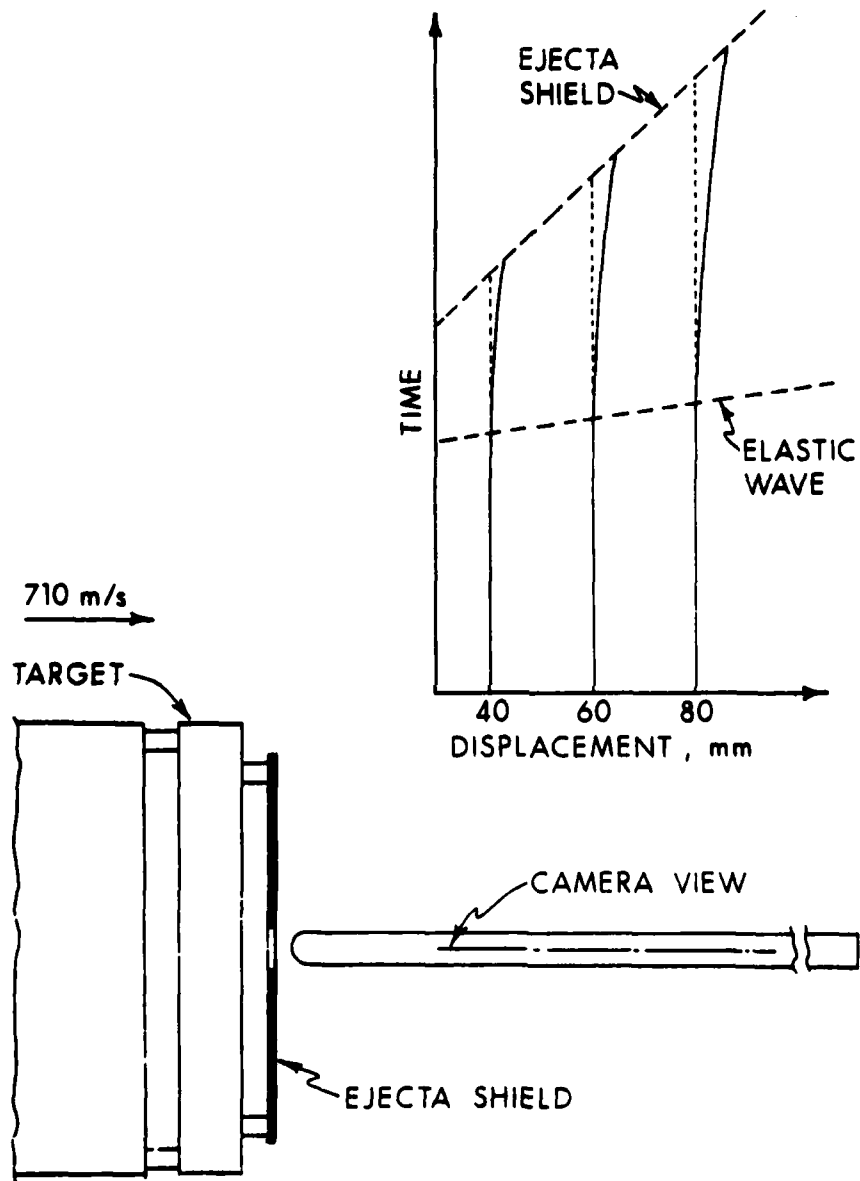


Figure 16. Reverse-ballistic arrangement used for optical measurements of rod displacement during penetration.

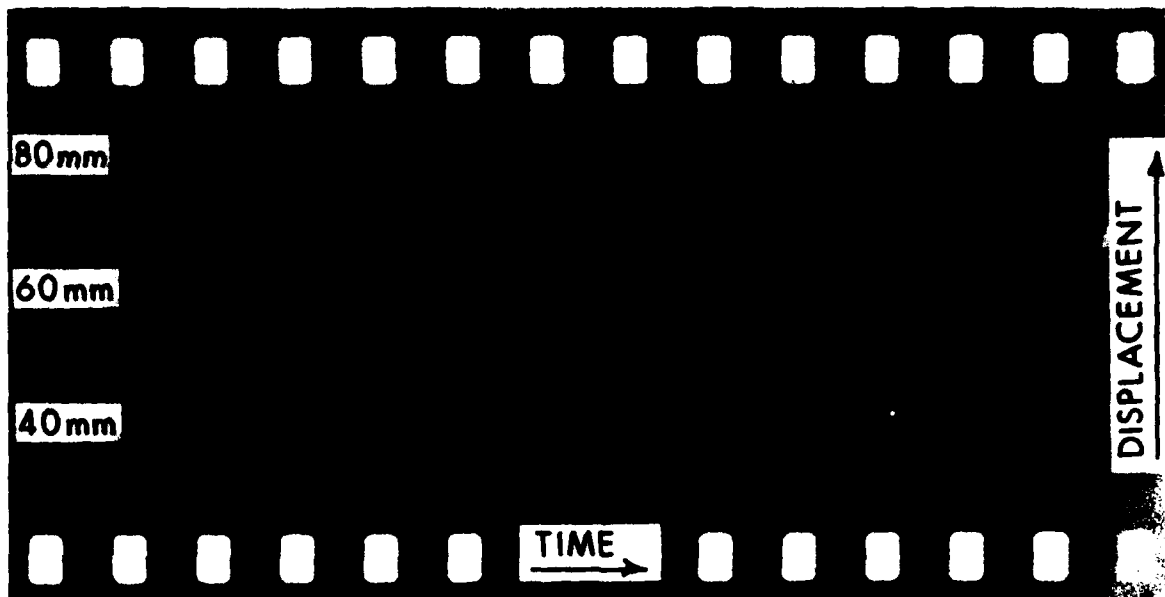


Figure 17. Photographic record of rod displacement during penetration (reverse-ballistic experiment).

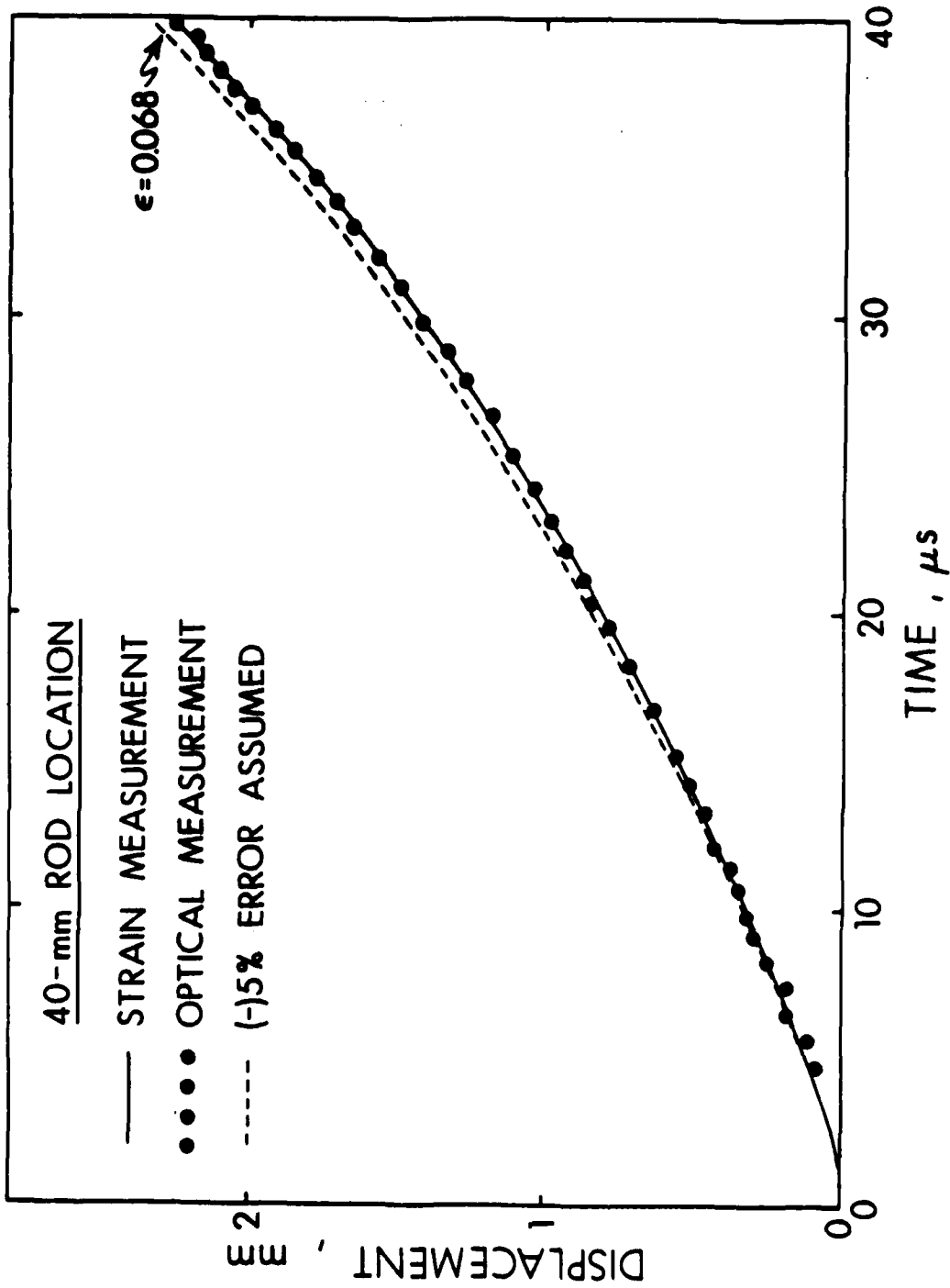


Figure 18. Displacement/time relationship, comparing displacement measured optically with displacement calculated from strain measurements.

this experiment was similar to the record shown in Figure 17, but continued to much larger displacements. As in the experiment at higher impact velocity, strain data were analyzed to provide displacements which could be compared with optical measurements of displacement. Figure 19 shows this comparison, again at the 40mm location on the rod. There is exact agreement at values of strain below 0.20. By strain of 0.23, the displacement based on strain data is clearly becoming smaller than the displacement measured optically. This is understandable because by strain of 0.23 the strain gage is clearly beginning to debond from the rod. In other experiments, measurements have continued to higher strains without evidence of debonding. Debonding certainly depends on a number of factors including gage size and surface preparation. In addition, it has been noted that gages are more resistant to debonding when the time between bonding and testing is short. The close agreement to strain of 0.20 provides additional confidence in the measurements of strain and in the simple-wave analysis which supplied the relationship between particle velocity and strain.

V. SUMMARY AND CONCLUSIONS

Both forward-ballistic and reverse-ballistic techniques are being used for strain measurements on long steel rods as they penetrate steel armor. Although forward ballistics imposes less severe limitations on the target size and impact velocity, the present state of the technique restricts the number of gages and the observation time, and produces data of somewhat lower quality than those obtained from reverse-ballistic experiments. Restricted targets of the reverse-ballistic technique have been accepted in order to achieve versatility and superior data during the preliminary efforts which are intended to develop a better understanding of dynamic rod behavior during penetration. The reliability of experimental data has been confirmed to strain of 0.20, and confidence in the analytical procedure was partially established since part of the procedure was successfully employed in the test of reliability.

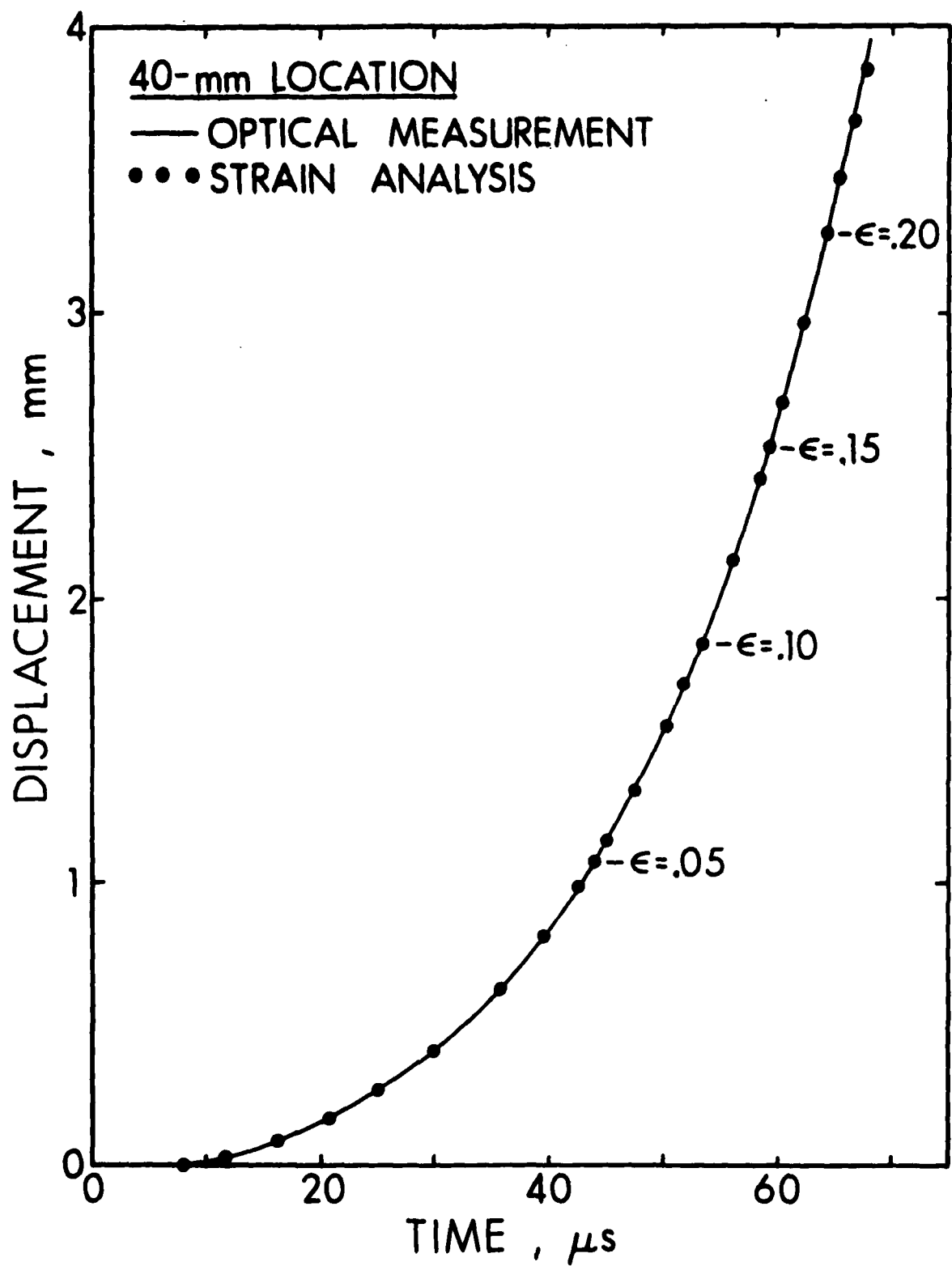


Figure 19. Comparison of displacements at the lower impact velocity of 450 m/s.

ACKNOWLEDGEMENTS

The authors gratefully acknowledge the general guidance and encouragement by T. W. Wright, and the contributions of J. F. Bell and J. Randall of The Johns Hopkins University whose impact experiments provided a comparison between strain measured by foil resistance gages and strain measured by ruled diffraction gratings.

REFERENCES

1. J. I. Bluhm, "Stresses in Projectiles During Penetration", Proc. Soc. Exptl. Stress Analysis, Vol. 13, 1956, pp. 167-182.
2. Visi Arajs, "An Investigation of Forces on a Projectile During Perforation of Thin Aluminum Plates", Masters Thesis, Air Force Inst. Tech., June 1971.
3. F. R. Lascher, D. Henderson, and D. Maynard, "Determination of Penetration Forcing Function Data for Impact Fuzes", Avco Systems Division, Wilmington, Mass., Technical Report AVSD-0306-75-RR, January 1975.
4. W. N. Sharpe, Jr., "Dynamic Plastic Response of Foil Gages", Experimental Mechanics, Vol. 10, No. 10, October 1970, pp 408-414.
5. J. F. Bell, "Propagation of Large Amplitude Waves in Annealed Aluminum", J. Applied Physics, Vol. 31, No. 2, February 1960, pp. 277-282.
6. M. H. Rice, "Calibration of the Power Supply for Manganin Pressure Gages", Air Force Weapons Laboratory Technical Report No. AFWL-TR-70-120, November 1970.
7. R. E. Franz, "Volume Changes in Metal Alloys Due to Plastic Deformation", Ballistic Research Laboratory Memorandum Report (In Preparation).

DISTRIBUTION LIST

<u>No. of Copies</u>	<u>Organization</u>	<u>No. of Copies</u>	<u>Organization</u>
12	Commander Defense Technical Info Center ATTN: DDC-DDA Cameron Station Alexandria, VA 22314	1	Commander US Army Aviation Research and Development Command ATTN: DRSAV-E P. O. Box 209 St. Louis, MO 63166
1	Director Defense Advanced Research Projects Agency ATTN: Tech Info 1400 Wilson Boulevard Arlington, VA 22209	1	Director US Army Air Mobility Research and Development Laboratory Ames Research Center Moffett Field, CA 94035
1	Deputy Assistant Secretary of the Army (R&D) Department of the Army Washington, DC 20310	1	Commander US Army Communications Rsch and Development Command ATTN: DRDCO-PPA-SA Fort Monmouth, NJ 07703
1	Commander US Army Materiel Development and Readiness Command ATTN: DRCMDM-ST 5001 Eisenhower Avenue Alexandria, VA 22333	1	Commander US Army Electronics Research and Development Command Technical Support Activity ATTN: DELSD-L Fort Monmouth, NJ 07703
2	Commander US Army Armament Research and Development Command ATTN: DRDAR-TSS (2 cys) Dover, NJ 07801	1	Commander US Army Harry Diamond Labs ATTN: DELHD-TA-L 2800 Powder Mill Road Adelphi, MD 20783
1	Commander US Army Armament Materiel Readiness Command ATTN: DRSAR-LEP-L, Tech Lib Rock Island, IL 61299	1	Commander US Army Missile Command ATTN: DRSMI-R Redstone Arsenal, AL 35809
1	Commander US Army Watervliet Arsenal ATTN: Dr. F. Schneider Watervliet, NY 12189	1	Commander US Army Missile Command ATTN: DRSMI-YDL Redstone Arsenal, AL 35809
1	Director US Army ARRADCOM Benet Weapons Laboratory ATTN: DRDAR-LCB-TL Watervliet, NY 12189		

DISTRIBUTION LIST

<u>No. of Copies</u>	<u>Organization</u>	<u>No. of Copies</u>	<u>Organization</u>
3	Commander US Army Mobility Equipment Research & Development Cmd ATTN: DRDME-WC DRSME-RZT STSFB-MW, Dr. J. Bond Fort Belvoir, VA 22060	1	Commander Naval Research Laboratory ATTN: Code 2020, Tech Lib Washington, DC 20375
		3	Commander Naval Surface Weapons Center ATTN: Mr. W. H. Holt Mr. W. Mock, Jr. DX-21, Lib Dahlgren, VA 22448
1	Commander US Army Tank Automotive Rsch and Development Command ATTN: DRDTA-UL Warren, MI 48090	2	Commander Naval Surface Weapons Center ATTN: Dr. J. W. Forbes Tech Lib Silver Spring, MD 20910
1	Director US Army TRADOC Systems Analysis Activity ATTN: ATAA-SL, Tech Lib White Sands Missile Range NM 88002	1	AFWL (Tech Lib) Kirtland AFB, NM 87117
5	Commander US Army Materiel and Mechanics Research Center ATTN: DRXMR-ATL DRXMR-H, Mr. J. Dignam DRXMR-H, Dr. D. Dandekar DRXMR-T, Dr. J. Mescall DRXMR-H, Dr. S. C. Chou Watertown, MA 02172	1	Director Lawrence Livermore Laboratory ATTN: Dr. M. van Thiel, L-64 P. O. Box 808 Livermore, CA 94550
		3	Sandia Laboratories ATTN: Tech Lib Dr. W. Herrmann Dr. L. D. Bertholf Albuquerque, NM 87115
1	Commander US Army Research Office P. O. Box 12211 Research Triangle Park NC 27709	3	SRI International ATTN: Dr. G. R. Abrahamson Dr. D. Curran Dr. L. Seaman 333 Ravenswood Avenue Menlo Park, CA 94025
1	Commander US Military Academy ATTN: Library West Point, NY 10996	1	Drexel Institute of Technology Wave Propagation Research Center ATTN: Prof. P. C. Chou 32nd and Chestnut Streets Philadelphia, PA 19104

DISTRIBUTION LIST

<u>No. of Copies</u>	<u>Organization</u>	<u>No. of Copies</u>	<u>Organization</u>
2	University of California Los Alamos Scientific Lab ATTN: Tech Lib GMX-6, Dr. J. W. Taylor P. O. Box 1663 Los Alamos, NM 87545	1	Washington State University Department of Physics ATTN: Prof. G. E. Duvall Pullman, WA 99163

Aberdeen Proving Ground

Dir, USAMSAA
ATTN: Dr. J. Sperrazza
DRXSY-MP, H. Cohen
Cdr, USATECOM
ATTN: DRSTE-TO-F
Dir, USACSL, Bldg. E3516
ATTN: DRDAR-CLB-PA

USER EVALUATION OF REPORT

Please take a few minutes to answer the questions below; tear out this sheet, fold as indicated, staple or tape closed, and place in the mail. Your comments will provide us with information for improving future reports.

1. BRL Report Number _____

2. Does this report satisfy a need? (Comment on purpose, related project, or other area of interest for which report will be used.)

3. How, specifically, is the report being used? (Information source, design data or procedure, management procedure, source of ideas, etc.) _____

4. Has the information in this report led to any quantitative savings as far as man-hours/contract dollars saved, operating costs avoided, efficiencies achieved, etc.? If so, please elaborate.

5. General Comments (Indicate what you think should be changed to make this report and future reports of this type more responsive to your needs, more usable, improve readability, etc.) _____

6. If you would like to be contacted by the personnel who prepared this report to raise specific questions or discuss the topic, please fill in the following information.

Name: _____

Telephone Number: _____

Organization Address: _____

FOLD HERE

Director
US Army Ballistic Research Laboratory
Aberdeen Proving Ground, MD 21005

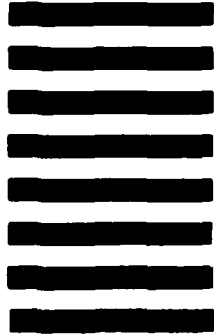


NO POSTAGE
NECESSARY
IF MAILED
IN THE
UNITED STATES

OFFICIAL BUSINESS

PENALTY FOR PRIVATE USE, \$300

BUSINESS REPLY MAIL
FIRST CLASS PERMIT NO 12062 WASHINGTON, DC
POSTAGE WILL BE PAID BY DEPARTMENT OF THE ARMY



Director
US Army Ballistic Research Laboratory
ATTN: DRDAR-TSB
Aberdeen Proving Ground, MD 21005

FOLD HERE

DATE
ILMED
-8